

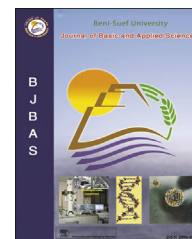
HOSTED BY



ELSEVIER

Available online at [www.sciencedirect.com](http://www.sciencedirect.com)

ScienceDirect

journal homepage: [www.elsevier.com/locate/bjbas](http://www.elsevier.com/locate/bjbas)

## Full Length Article

# Synthesis, characterization and fabrication of gas sensor devices using ZnO and ZnO:In nanomaterials

H. Shokry Hassan <sup>a,\*</sup>, A.B. Kashyout <sup>a</sup>, I. Morsi <sup>b</sup>, A.A.A. Nasser <sup>b</sup>, Ibrahim Ali <sup>b</sup><sup>a</sup> Electronic Materials Researches Department, Advanced Technology and New Materials Researches Institute, City of Scientific Research and Technological Applications, New Borg El-Arab City, Alexandria 21934, Egypt<sup>b</sup> Arab Academy for Science, Technology and Maritime Transport, Alexandria 21934, Egypt

## ARTICLE INFO

## Article history:

Received 26 August 2014

Received in revised form

15 September 2014

Accepted 25 September 2014

Available online 10 November 2014

## Keywords:

ZnO nanorods

Morphological structures

Gas sensor devices

Dopant elements

sol–gel

## ABSTRACT

Undoped and In-doped ZnO including nanoparticles and nanorods were successfully synthesized via sol gel method. Effect of different doping ratios (1, 5 and 10%) of indium as a dopant element was optimized for the highest gas sensitivity. The morphological structures of prepared Undoped and doped ZnO were revealed using scanning electron microscope (SEM) and the aspect ratios of nanorods were calculated. X-ray diffraction (XRD) patterns reveal a highly crystallized wurtzite structure and used for identifying phase structure and chemical state of both ZnO and ZnO doped with In under different doping ratios. Energy dispersive X-ray (EDS) analysis was performed to be confirming the chemical composition of the In-doped ZnO nanopowders. The gas sensitivity for O<sub>2</sub>, CO<sub>2</sub> and H<sub>2</sub> gases were measured for the fabricated gas sensor devices as a function of temperature for In-doped ZnO nanopowders and compared with un-doped ZnO films.

Copyright 2014, Beni-Suef University. Production and hosting by Elsevier B.V. All rights reserved.

## 1. Introduction

Semiconductor gas sensors present the property of changing the conductivity of the sensing material in presence of a determinate gas. The working temperature at which these devices are more efficient can vary depending on the gas atmosphere and on properties of the sensor material selected in every case (Seiyama et al., 1962).

Metal oxide semiconductor gas sensors have attracted a lot of attention due to their cheap and easy-to-use gas monitoring capabilities. It is consist of three main components sensing material, electrodes, and a heater. The commonly used sensing materials include SnO<sub>2</sub>, WO<sub>3</sub>, ZnO or In<sub>2</sub>O<sub>3</sub> (Gong, 2005).

Zinc oxide is an interesting II–VI compound semiconductor with a wide band gap of 3.37 eV and a large exciton

\* Corresponding author. Tel.: +20 1282305425; fax: +20 3 4593414.

E-mail addresses: [hassan.shokry@gmail.com](mailto:hassan.shokry@gmail.com) (H. Shokry Hassan), [hady8@yahoo.com](mailto:hady8@yahoo.com) (A.B. Kashyout), [drimanmorsi@yahoo.com](mailto:drimanmorsi@yahoo.com) (I. Morsi), [menem\\_1954@yahoo.com](mailto:menem_1954@yahoo.com) (A.A.A. Nasser), [abrs\\_218@yahoo.com](mailto:abrs_218@yahoo.com) (I. Ali).

Peer review under the responsibility of Beni-Suef University.

<http://dx.doi.org/10.1016/j.bjbas.2014.10.007>

2314-8535/Copyright 2014, Beni-Suef University. Production and hosting by Elsevier B.V. All rights reserved.

binding energy of 60 meV (Greene et al., 2006). Polycrystalline ZnO used in multiple application such as ultraviolet (UV) light emitters, short-wavelength nano-lasers, piezoelectric devices, ultrasensitive, spin electronics, gas sensor, field-effect transistors, and field emitters (Wang, 2007). ZnO gas sensor has a good characteristic like chemical sensitivity to different adsorbed gases, amenability to doping, high chemical stability, non-toxicity, and low cost. ZnO is still attractive due to its easy fabrication in thin film form with various methods (Fawzy and Kiriakidis, 2009; Dong et al., 1997; Basu and Dutta, 1997) and its improved sensor performance by addition of dopants (Arshak et al., 2004; Watson, 94).

Hydrolysis, condensation and drying are three key steps in determining the properties of the final product in sol–gel processing (Kenneth, 2001). Sol–gel processes have several advantages over other techniques for synthesizing nanopowders of metal oxides. These include the production of ultrafine porous powders and homogeneity of the product as a result of homogenous mixing of the starting materials on the molecular level. Also, sol–gel processing holds strong promise for employment industrially on large scales (Shokry Hassan et al., 2013). In this work we have chosen sol–gel technique for the previous advantages.

## 2. Materials and methods

### 2.1. Preparation of ZnO and ZnO:In nanopowders and films fabrication

A 0.1 M of zinc chloride  $ZnCl_2$  has been prepared by distilling 3.4 g of zinc chloride in 250 ml distilled water. A magnetic stirrer is incorporated for this purpose for about 10–15 min. Increase the pH for the solution to be 9 by adding  $NH_3OH$  to the solution. For preparation of 1, 5 and 10 wt% In-doped ZnO; an equivalent amount of indium chloride is added to the mixture. Then the mixture was stirred at 80 °C in a glass beaker for 24 h (Shokry Hassan et al., 2014a, b). ZnO white powders were separated and washed many times using ethanol and distilled water. The final product was centrifuged at 6000 rpm for 30 min, and then dried under atmospheric air.

### 2.2. Preparation and characterization of solid state gas sensor devices

Solid state gas sensor device was obtained as the following: colloidal suspension was obtained by mixing the synthesized ZnO nanopowder either doped or un-doped with ethanol and stirring the resulting suspension overnight. Ethanolic solution with ZnO content of about 20% by weight was attended. Sputtering machine (Turbo Sputtering RF & DC Power Supplies Deposition System Model Hummer 8.1) ( $P = 100$  W RF,  $t = 5$  min) was used to deposit platinum heater onto the previously cleaned glass substrate. ZnO suspension was deposited using wafer spinner machine (100 rpm, 2 min) (Model Polos300 AWS), and then the film was dried in air. The ZnO films were sintered shortly after deposition in air flow at 400 °C for 5 min. Pt contact electrodes were deposited by sputtering machine ( $P = 100$  W RF,  $t = 2$  min) on the front

surface of the ZnO film. The fabricated cell of gas sensor device was inserted inside the homemade gas chamber. Different gases ( $O_2$ ,  $CO_2$ , and  $H_2$ ) were passed inside the gas chamber through opening the chamber valve. The resistivity of the gas sensor device was measured and the resultant sensitivity was plotted against the studied gas temperature for all gases. The sensor response was defined as the ratio ( $S = R_d/R_g$ ) of the resistance of the sensor in dry air ( $R_d$ ) to that in target gases ( $R_g$ ) at each temperature.

### 2.3. Characterization of ZnO and ZnO doped with In nanopowders

All the samples were characterized by x-ray diffraction using Shimadzu 7000 Diffractometer operating with  $CuK\alpha$  ( $\lambda = 0.15406$  nm) with scan rate of  $2^\circ \text{ min}^{-1}$  for  $2\theta$  values between  $20^\circ$  and  $80^\circ$ . Morphological structures and size distribution of ZnO:In nanopowders were investigated by scanning electron microscopy (SEM) (JEOL JSM 6360LA, Japan). Energy dispersive X-ray analysis (EDS) was employed to perform the chemical composition of the ZnO:In nanomaterials.

## 3. Results and discussion

### 3.1. Effect of In doping process on ZnO nanomaterials characteristics

Fig. 1 shows the SEM micrographs of pure ZnO, ZnO:In with 1%, 5%, and 10% weight ratios respectively. That Indium presence in any ratio changes the morphological structure from a uniform nanorods to nanoparticles. It is clear that, the ZnO nanostructures depended on the doping ratio. For pure ZnO, well-formed nanorods structures with average length of 5  $\mu\text{m}$  and a diameter of 300 nm have been predominated (Fig. 1(a)). With starting doping process with In doping ratio 1%, ZnO nanorods come to be shorter in length and the diameters increase as shown in Fig. 1(b). Increasing in doping ratio of In to be 5% leads to the ZnO nanorods convert to elongated nanoparticles, then to spherical nanoparticles with 10% In doping ratio respectively (Fig. 1(c and d)). It implies that In have an important effect on the crystallization and growth of ZnO nanoparticles (Rozati et al., 2011).

All of the diffraction peaks can be indexed to be those of hexagonal wurtzite structured ZnO as shown in Fig. 2(1) which agrees well with those given in relevant XRD database (JCPDS card No. 01-089-1397). No characteristic peaks of other impurities are observed, which indicates that In is incorporated in zinc oxide matrix via substituting  $Zn^{2+}$ . Besides, there exists a minor difference in the pattern and intensity of the (100), (002) and (101) peaks of various In doped ZnO nanopowder samples with different concentrations of In dopant (Fig. 2(2, 3, 4)), which implies that the effect of In dopant on the crystal structure, and grain size of as-synthesized ZnO/In nanostructures is concentration-dependent (Kow-Ming et al., 2011).

Fig. 3(a–c) shows the energy dispersive X-ray analysis (EDS) of ZnO nanopowder doped with 1, 5, 10% wt In. According to Table 1, In weight ratio in nanopowders as detected

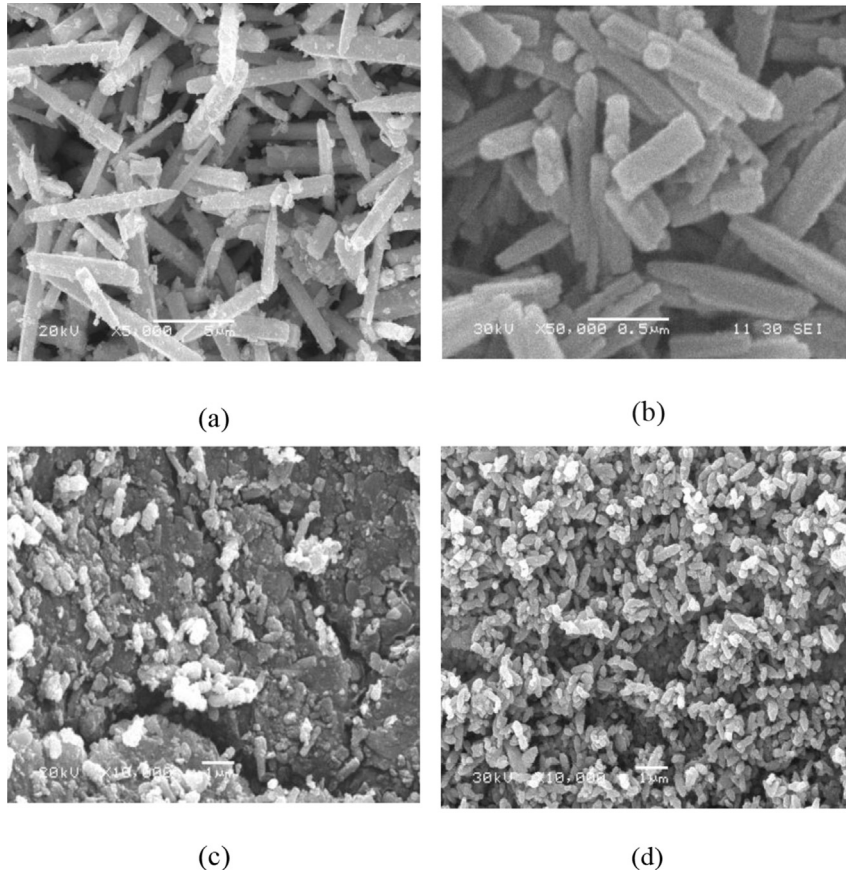


Fig. 1 – SEM micrographs of (a) pure ZnO, (b) ZnO:In = 99:1, (c) ZnO:In = 95:5, (d) ZnO:In = 9:1.

by (EDS) analysis is 1.19%, which is in accordance with the starting In amount in the solution (1%). The weight ratio resulted in the starting weight ratio of In (5%) is 4.95% as shown in Table 2. Table 3 shows EDS of ZnO nanoparticles doped with 10 wt % of In which resulted in 9.91%. All results are indicating to the actual starting In element.

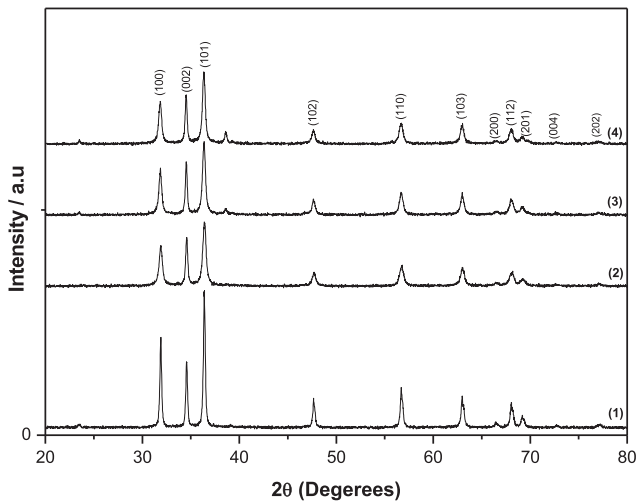


Fig. 2 – XRD patterns of ZnO nanoparticles: (1) pure ZnO, (2) ZnO:Al = 99:1, (3) ZnO:Al = 95:5, (4) ZnO:Al = 9:1.

### 3.2. Gas sensing performance for ZnO:In gas sensor devices

Gas sensor devices were fabricated as semiconductor gas sensor (SGS) and tested for the same different concentration (100 ppm) of gases. Furthermore, different doped ZnO samples were applied as gas devices to determine the optimum dopant element and its proper doping weight ratios for high gas sensitivity. It's known that the gas response "S" is given by the Eq. (1)

$$S = \frac{R_a}{R_g} \times 100 \quad (1)$$

where  $R_a$  and  $R_g$  express the resistance of the sensor in air and in tested gas, respectively. The effect of the temperature on gas sensitivity of the fabricated devices for the several studied analytic gases was measured as a function of their electrical resistance.

For  $O_2$  gas, it can be observed, from the respective dependences that, the sensitivity increases with increasing working temperature, reach a maximum value (from 150 to 250 °C, which considered low working temperature) and then falls with further increase in operating temperature (Fig. 4). Also, it is clear that, the highest sensitivity is about 74% For  $H_2$  gas, it's observed that, the maximum sensitivity is about 93% as shown in Fig. 5.  $CO_2$  gas sensor presents the lowest gas sensitivity, which attained to 16% sensitivity, which consider poor sensitivity (Fig. 6).

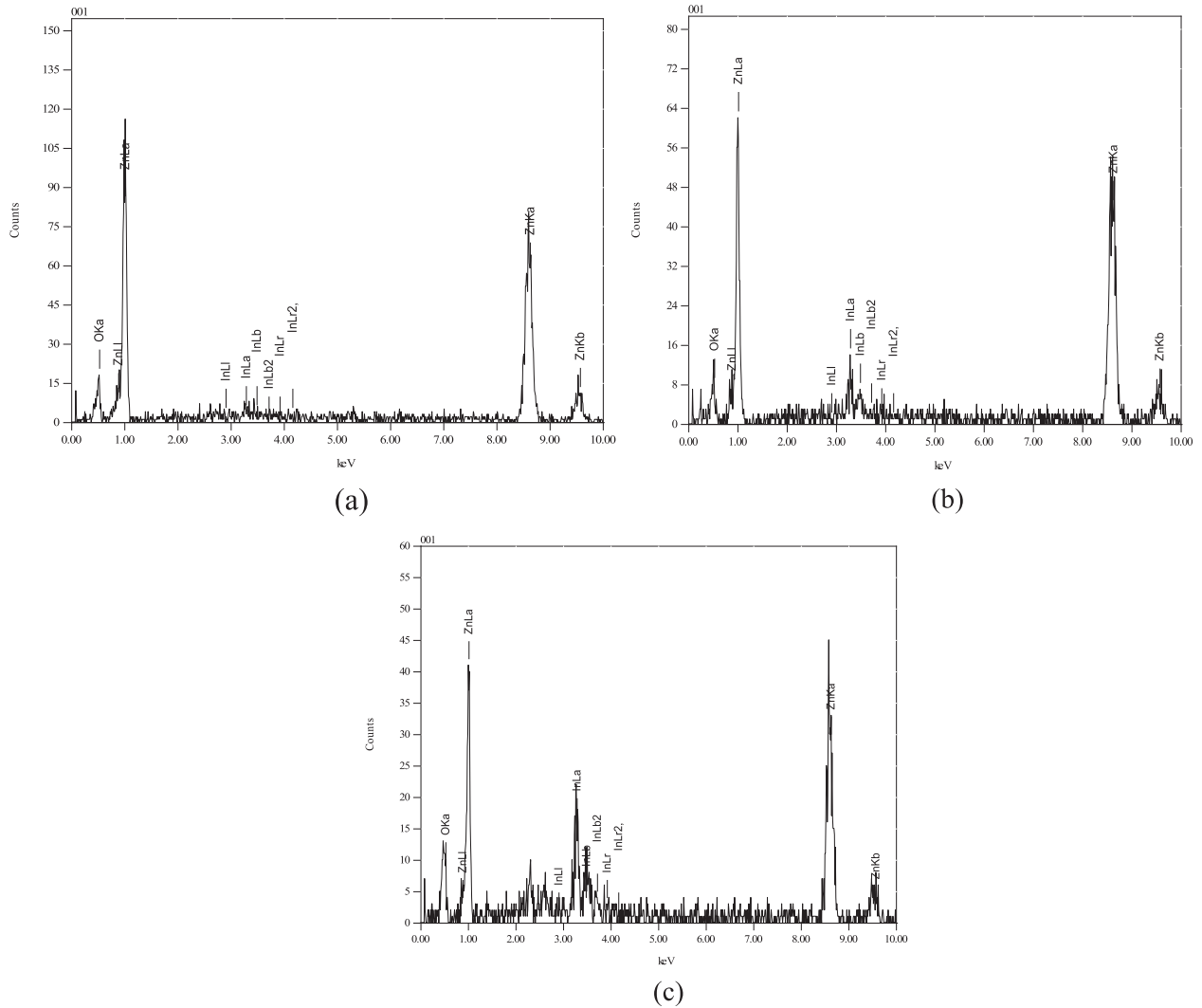


Fig. 3 – EDS Spectra of ZnO doped with (a) 1%, (b) 5% and (c) 10% wt In.

Actually, gas sensing mechanism is based on the surface reactions between the tested gas and adsorbed oxygen. Atmospheric oxygen molecules are adsorbed on the surface of n-type semiconductor oxides in the forms of  $O^-$  and  $O^{2-}$ . It depletes electrons from the conduction band (Shokry Hassan et al., 2014a, b; Zhang et al., 2008). When negatively charged oxygen reacts with the tested molecules, the trapped electrons are given back to conduction band of investigated semiconductor oxides. The thermal energy will increase by increasing the operating temperature to stimulate the oxidation of the tested gases ( $O_2$ ,  $H_2$  and  $CO_2$ ). On the other hands, the reducing gas ( $H_2$ ) donates electrons to the investigated SGS films; therefore the resistance decreases (Rambu et al., 2013;

Kashyout et al., 2010). When the operation temperature is increasing to higher value, the gas sensitivity is decreasing. This is because of the oxygen molecules which are desorbed from the surface of the sensor (Windichmann & Mark, 1979).

Instead, for In:ZnO films, the sensitivity values increase, by comparison with pure ZnO. For investigated films, an increase of sensitivity with the increase of In concentration in ZnO host is observed. The main influence of doping process is for enhancement the electrical properties. It well known that, gas sensing properties is improved in the case of doped materials, mixed materials, etc. This process leads to an increase of the electron concentration, which eventually increases the conductivity of the ZnO/In gas sensor. The sensitivity of carbon

Table 1 – The EDS analysis of ZnO doped with 1% wt In.

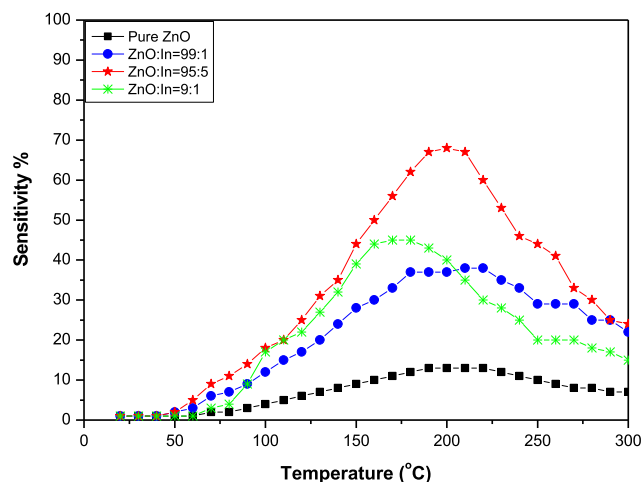
Element	(keV)	Mass%	Error%	At%	K
O	0.525	5.68	0.17	19.89	5.2553
Zn	8.630	92.33	0.81	79.14	92.9040
In	3.230	1.99	0.43	0.79	1.8407
Total		100.00		100.00	

Table 2 – The EDS analysis of ZnO doped with 5% wt In.

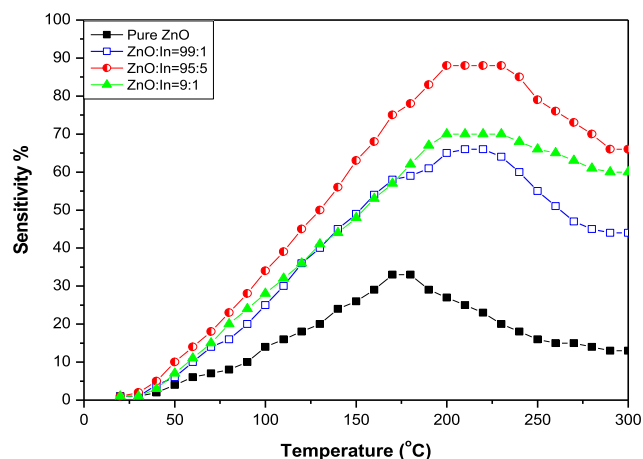
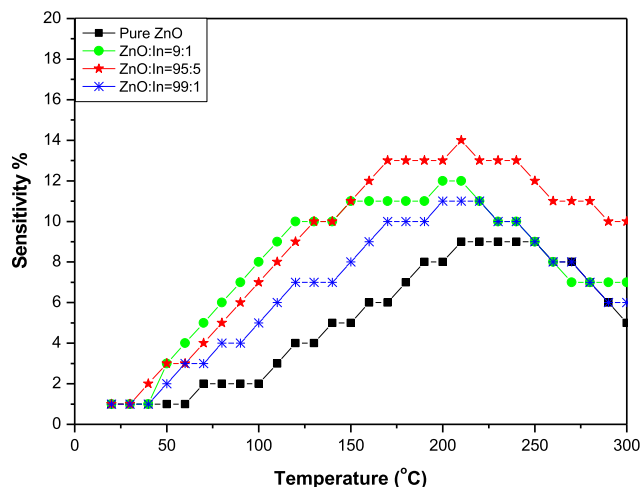
Element	(keV)	Mass%	Error%	At%	K
O	0.525	4.00	0.18	15.01	3.3291
Zn	8.630	88.80	0.80	80.85	89.2485
In	3.230	7.92	0.42	4.14	7.4245
Total		100.00		100.00	

**Table 3 – The EDS analysis of ZnO doped with 10% wt In.**

Element	(keV)	Mass%	Error%	At%	K
O	0.525	5.88	0.29	21.93	4.1054
Zn	8.630	74.15	1.04	67.69	76.4435
In	3.230	19.97	0.54	10.38	19.4511
Total		100.00		100.00	

**Fig. 4 – Sensitivity of ZnO doped and undoped gas sensor measured as a function of temperature for O<sub>2</sub>.**

dioxide gas on the fabricated ZnO gas sensors is attributed to the chemisorption of oxygen on the sensor surface and the subsequent reaction between adsorbed oxygen anion species and the CO<sub>2</sub> gas. Consequently, when ZnO gas sensor is exposed to a carbon dioxide gas atmosphere, CO<sub>2</sub> molecules react with the pre-adsorbed oxygen species. As a result, the surface oxygen concentration is reduced, and electrons that were initially trapped by oxygen anions are released back into the ZnO solid, leading to an increase in the conductivity of the sensor. The reaction of CO<sub>2</sub> with adjacent pairs of oxygen anions produced surface bidentate carbonate species. The adsorption of CO<sub>2</sub> at a single oxygen anion site then yields

**Fig. 5 – Sensitivity of ZnO doped and undoped gas sensor measured as a function of temperature for H<sub>2</sub>.****Fig. 6 – Sensitivity of ZnO doped and undoped gas sensor measured as a function of temperature for CO<sub>2</sub>.**

surface carboxylate groups. During the formation of all these surface species, there is no electron transfer to the bulk metal oxide sensor, thus no conductance change. However desorption of CO<sub>3</sub> provides opportunities for the electrons to return to the sensor solid. Furthermore, desorption of the formed CO<sub>3</sub> is favored at higher temperatures, but not favored at low temperatures (Zhao et al., 2013).

For the ZnO sensors, In doping leads to the introduction of more oxygen vacancies-related defects in ZnO nanoparticles. Therefore, more adsorption sites for gas molecules are provided by these oxygen vacancies causing the surface to become highly active for reaction (Shokry Hassan et al., 2013), so that the sensing properties are improved.

#### 4. Conclusions

In-doped and pure ZnO films were fabricated by a sol-gel process with different In doping concentrations using zinc nitrate as the starting materials. The microstructure and electrical properties of In-doped ZnO films were investigated as a function of doping concentrations. For oxygen gas, the best doping ratio that has a maximum oxygen sensitivity was recorded at Zn/In = 95:5 at temperature about 150–250 °C. The fabricated gas sensor devices attain low carbon dioxide gas response, where the maximum CO<sub>2</sub> sensitivity recorded for the In doped ZnO gas sensors with dopant ratio for ZnO:In of 95:5 that equal 16% and achieved at 200 °C. The highest sensitivity values for both pure ZnO and doped ZnO gas sensor with In element established for H<sub>2</sub>. The maximum sensitivity is given at Zn:In = 95:5 weight ratio, that get to 93% at temperature value around 190 °C.

#### REFERENCES

Arshak K, Moore E, Lyons GM, Harris J, Clifford S. A review of gas sensors employed in electronic nose applications. *Sens Rev* 2004;24:181–218.



- Basu S, Dutta A. Room temperature hydrogen sensors based on ZnO. *Mater Chem Phys* 1997;47:93–6.
- Dong LF, Cui ZL, Zhang ZK. Gas sensing properties of nano-ZnO prepared by arc plasma method. *Nano Struct Mater* 1997;8:815–23.
- Fawzy A, Kiriakidis G. Nanocrystalline ZnO thin film for gas sensor application. *J Ovonic Res* 2009;5:15–20.
- Gong J. Non-silicon microfabricated nanostructured chemical sensors for electronic nose application. University of Central Florida; 2005.
- Greene LE, Yuhua BD, Law M, Zitoun D, Yang P. *Inorg Chem* 2006;45:7535–43.
- Kashyout AB, Soliman HMA, Shokry Hassan H, Abousehly AM. Fabrication of ZnO and ZnO:Sb nanoparticles for gas sensor applications. *J Nanomater* 2010. ID341841:8 Pages.
- Kenneth J. In: Klabunde, editor. *Nanoscale materials in chemistry*; 2001. p. 110–5. New York, Chichester, Weinheim, Singapore, Brisbane, Toronto.
- Kow-Ming C, Sung-Hung H, Chin-Jyi W, Wei-Li L, Wei-Chiang C, Chia-Wei C, et al. Transparent conductive indium-doped zinc oxide films prepared by atmospheric pressure plasma jet. *Thin Solid Films* 2011;519:5114–7.
- Rambu AP, Ursu L, Iftimie N, Nica V, Dobromir M, Iacomi F. Study on Ni-doped ZnO films as gas sensors. *Appl Surf Sci* 2013;280:598–604.
- Rozati SM, Zarenejad F, Memarian N. Study on physical properties of indium-doped zinc oxide deposited by spray pyrolysis technique. *Thin Solid Films* 2011;520:1259–62.
- Seiyama T, Kato A, Fujisishi K, Nagatoni M. A new detector for gaseous components using semiconductive thin films. *Anal Chem* 1962;34:1052–3.
- Shokry Hassan H, Kashyout AB, Soliman HMA, Uosif MA, Afify N. Effect of reaction time and Sb doping ratios on the architecturing of ZnO nanomaterials for gas sensor applications. *Appl Surf Sci* 2013;277:73–82.
- Shokry Hassan H, Kashyout AB, Morsi I, Nasser AAA, Raafat A. Fabrication and characterization of gas sensor micro-arrays. *Sens Biosens Res* 2014a;1:34–40.
- Shokry Hassan H, Elkady MF, El-Shazly A, Bamufleh Hisham S. Formulation of synthesized zinc oxide nanopowder into hybrid beads for dye separation. *J Nanomater* 2014. ID 967492:14 Pages.
- Wang ZL. Novel nanostructures of ZnO for nanoscale photonics, optoelectronics, piezoelectricity, and sensing. *Appl Phys A: Mater Sci Process* 2007;88:7–15.
- Windichmann H, Mark P. A model for the operation of a thin films SnO<sub>x</sub> conductance modulation carbon dioxide sensor. *J Electrochem Soc* 1979;126:627–33.
- Zhang N, Yu K, Li L, Zhu Z. Investigation of electrical and ammonia sensing characteristics of Schottky barrier diode based on a single ultra-long ZnO nanorod. *Appl Surf Sci* 2008;254:5736–40.
- Zhao M, Wang X, Cheng J, Zhangc L, Jia J, Li X. Synthesis and ethanol sensing properties of Al-doped ZnO nanofibers. *Curr Appl Phys* 2013;13:403–7.